



## ORIGINAL ARTICLE

# Synthesis, in vitro thymidine phosphorylase inhibitory activity and molecular docking study of novel pyridine-derived bis-oxadiazole bearing bis-schiff base derivatives



Rafaqat Hussain <sup>a</sup>, Wajid Rehman <sup>a,\*</sup>, Fazal Rahim <sup>a</sup>, Shoaib Khan <sup>a</sup>,  
Ashwag S. Alanazi <sup>b</sup>, Mohammed M. Alanazi <sup>c</sup>, Liaqat Rasheed <sup>a</sup>, Yousaf Khan <sup>d</sup>,  
Syed Adnan. Ali. Shah <sup>e,f</sup>, Muhammad Taha <sup>g</sup>

<sup>a</sup> Department of Chemistry, Hazara University, Mansehra 21120, Pakistan

<sup>b</sup> Department of Pharmaceutical Sciences, College of Pharmacy, Princess Nourah bint Abdulrahman University, P.O. Box 84428, Riyadh 11671, Saudi Arabia

<sup>c</sup> Department of Pharmaceutical Chemistry, College of Pharmacy, King Saud University, P.O. Box 2457, Riyadh 11451, Saudi Arabia

<sup>d</sup> COMSATS Department of Chemistry, COMSATS University, Islamabad, Pakistan

<sup>e</sup> Faculty of Pharmacy, Universiti Teknologi MARA Cawangan Selangor Kampus Puncak Alam, Bandar Puncak Alam 42300, Selangor, Malaysia

<sup>f</sup> Atta-ur-Rahman Institute for Natural Product Discovery (AuRIns), Universiti Teknologi MARA Cawangan Selangor Kampus Puncak Alam, Bandar Puncak Alam 42300, Selangor, Malaysia

<sup>g</sup> Department of Clinical Pharmacy, Institute for Research and Medical Consultations (IRMC), Imam Abdulrahman Bin Faisal University, P.O. Box 1982, Dammam 31441, Saudi Arabia

Received 11 January 2023; accepted 28 February 2023

Available online 6 March 2023

## KEYWORDS

Synthesis;  
Molecular docking;  
Thymidine Phosphorylase;  
Oxadiazole

**Abstract** The current study has afforded twelve analogs (**4a-l**) of pyridine-derived bis-oxadiazole containing bis-schiff base and subsequently evaluated for their potential to inhibit thymidine phosphorylase (in vitro). All the synthesized analogs were structurally elucidated using various spectroscopic tools including NMR and HREIMS. All synthesized scaffolds showed varied range of inhibitory potential with IC<sub>50</sub> values ranging from 5.19 ± 1.10 to 36.18 ± 4.60 μM in comparison to 7-deazaxanthine (IC<sub>50</sub> = 30.28 ± 2.10 μM) as a standard drug. All analogs (except analog **4l** which displayed less potency than standard drug) showed improved potency having IC<sub>50</sub> values of 19.73 ± 2.30, 16.14 ± 1.20, 18.93 ± 1.60, 22.78 ± 1.80, 30.47 ± 3.70, 5.19 ± 1.10, 23.13 ± 1.90, 21.56 ± 2.50, 4.88 ± 1.10, 26.63 ± 2.90 and 6.67 ± 1.10 respectively. Results obtained were compared to standard 7-deazaxanthine drug with IC<sub>50</sub> values of 30.28 ± 2.10 μM. Structure-activity relationship (SAR) studies revealed that analogs bearing -NO<sub>2</sub>, -CF<sub>3</sub>, -OH and -Cl moieties at various position of aryl part showed many folds more potency than standard 7-deazaxanthine standard

\* Corresponding author.

E-mail address: [sono\\_waj@yahoo.com](mailto:sono_waj@yahoo.com) (W. Rehman).

drug. In order to determine the potential mode of interactions with thymidine phosphorylase active sites, the most active analogs **4f** (bearing 3-CF<sub>3</sub>& 5-NO<sub>2</sub>), **4i** (bearing 3-OH & 5-NO<sub>2</sub>), and **4k** (bearing 2-OH & 5-NO<sub>2</sub>) were further subjected to molecular docking study. The results confirmed that these active analogs adopted numerous important interactions including hydrogen bonding, pi-donor hydrogen bond, pi-pi T shaped, pi-pi stacking, pi-alkyl, pi-anion, pi-sigma, halogen (fluorine) and numerous Vander Waals interactions with the amino acid of enzyme being targeted.

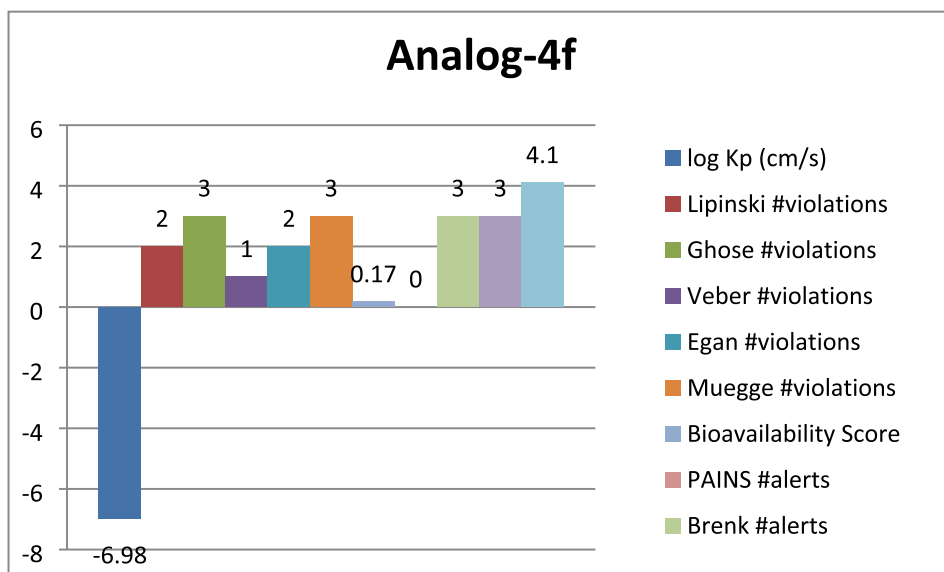
© 2023 The Author(s). Published by Elsevier B.V. on behalf of King Saud University. This is an open access article under the CC BY-NC-ND license (<http://creativecommons.org/licenses/by-nc-nd/4.0/>).

## 1. Introduction

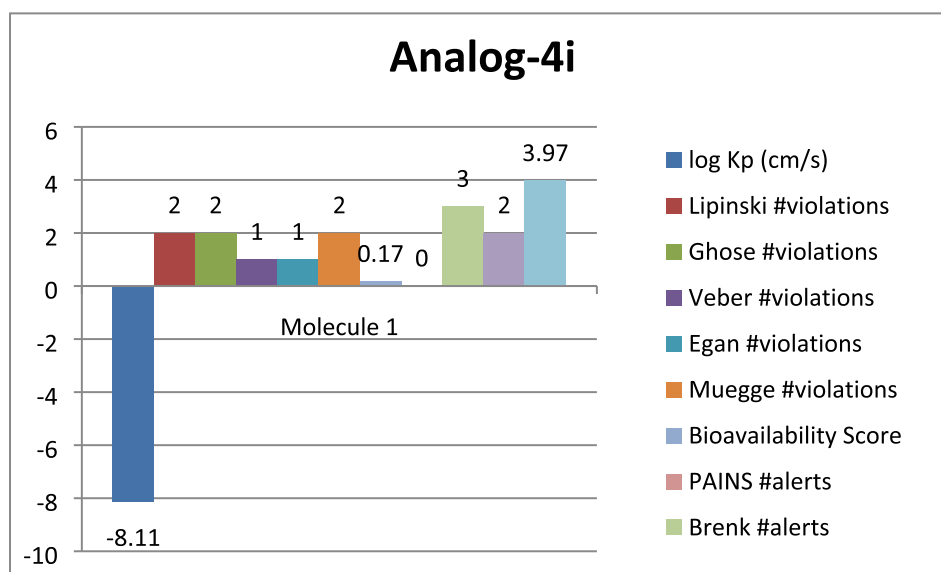
Human thymidine phosphorylase (HTP) acts in pathway of pyrimidine salvage to restore the nucleotides of pyrimidine necessary for replication of DNA and repair (Friedkin and Roberts 1954). In the presence of inorganic phosphates, this enzyme functions as catalyst the reversible reaction of thymidine phosphorylation (dThd) to deliver 2DDR-1P (2-deoxy-D-ribose-1-phosphate) and thymine. Additionally, hTP exhibits de-oxyribosyl transferase profile, which results in the creation of new pyrimidine nucleosides by moving the de-oxyribosyl moiety from one pyrimidine base to another (Schwartz 1971, Iltzsch et al., 1985). It has been demonstrated that the two proteins are linked, with hTP specifically sharing sequence of an amino acid with PD-ECGF (growth factor of platelet obtained endothelial cell) and gliostatin. While PD-ECGF has been shown to angiogenesis promotion, gliostatin is thought to regulate the proliferation of glial cells (Asai et al., 1992; Moghaddam and Bicknell 1992; Usuki et al. 1992). Since different types of tumours express hTP at higher levels than normal human tissues do; it appears to be crucial in the aetiology of cancer. The enzyme has generally been found to be present in higher concentrations in tissues that have been exposed to radio- and chemotherapeutic circumstances, stressful conditions of microenvironments and the different inflammatory cytokines existence including low pH and hypoxia (Brown et al. 2000). Elevated levels of hTP are mostly linked with poor prognosis and aggressiveness of cancer because of its anti-apoptotic and pro-angiogenic features (Moghaddam et al. 1995; Matsuura et al. 1999; Ikeda et al. 2003). It has been discovered that one of the by hTP catalyzed enzymatic reaction's products is connected to the pro-tumor signalling mechanism. After the N-glycosidic link is broken, 2DDR-1P is

produced, and non-enzymatic de-phosphorylation transforms it into 2-deoxy-D-ribose (2DDR). 2DDR initiates angiogenic and anti-apoptotic actions as it leaves the cell (Haraguchi et al. 1994; Miyadera et al. 1995; Liekens et al. 2002). Through the stimulation of the integrin downstream signalling cascade, this chemical influences endothelial cell motility. Additionally, through boosting the production and/or secretion of numerous factors of angiogenic, including interleukins (ILs), matrix metalloproteinases (MMPs), and VEGF (growth factor of vascular endothelial), the tumor microenvironment encourages cancer and angiogenesis spread (Hotchkiss et al. 2003; Bijnsdorp et al. 2011; de Moura Sperotto et al. 2019). A correlation between hTP and 2DDR and resistance to hypoxia-induced apoptosis in various tumor cell types has also been found. Moreover, 2DDR and hTP have been correlated with protection against apoptosis in different types of tumours cell by hypoxia induction. Either 2DDR or hTP inhibited hypoxia-induced pro-apoptosis signals via several mechanisms, such as activation of caspase-3 and caspase-9, up-regulation of HIF-1, BCL-XL and BCL<sub>2</sub> down-regulation, mitochondrial transmembrane potential reduction, HIF-1  $\alpha$  up-regulation and mitochondrial cytochrome-C release (Ikeda et al. 2002; Jeung et al. 2005; Jeung et al. 2006). Graph 1. Graph 2. Graph 3.

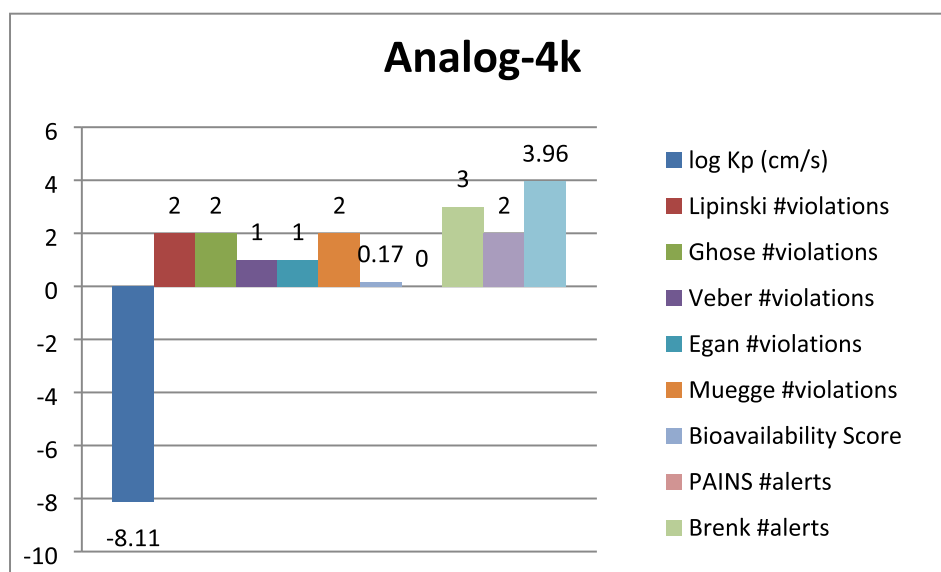
Oxadiazole analogs find application in diverse medicinal fields owing to its broad range of biological and pharmaceutical profile among the five-membered aromatic heterocyclic compounds (Katritzky et al. 2010). Oxadiazole-based scaffolds were reported to demonstrate interesting biological potentials such as antiviral (Du and Luo 2010), antimicrobial (Salar et al. 2015; Zheng et al. 2018), antihypertensive (Zhu et al. 2016), anti-inflammatory (Palaska et al. 2002), anticonvulsant (Dogana et al. 2002), analgesic



**Graph 1** Represent the ADMET prediction of analog-4f. Analog-4i was found with most effective properties such as logP = -8.11 cm/s, Lipinski violations = 2, Ghose violations = 2, veber violation = 1, Egan violation = 1, Muegge violation = 2, Bioavailability score = 0.17, pain alert = 0 Brenk alerts = 3 etc.



**Graph 2** Represent the ADMET prediction of analog-4i. Analog-4 k was found with most effective properties such as logP = -8.11 cm/s, Lipinski violations = 2, Ghose violations = 2, veber violation = 1, Egan violation = 1, Muegge violation = 2, Bioavailability score = 0.17, pain alert = 0 Brenk alerts = 3 etc.



**Graph 3** Represent the ADMET prediction of analog-4 k.

(Husain et al. 2009), antidiabetic (O'Neal et al. 1962), antitubercular activities (Pattan et al. 2009) and anti-leishmanial (Taha et al. 2017). Oxadiazole scaffolds gained much attention to medicinal chemists owing to its broad application in the treatment of HIV infections (El-Emam et al. 2004) and cancer (Shivarama et al. 2005). Additionally, in development of more biologically potent drugs, oxadiazole had been employed as bioisosteres for amide, ester and carboxylic acid functional groups (Orlek et al. 1991; Omar et al. 1996; Leung et al. 2005). Many marketed drugs contain oxadiazole nucleus such as nesapidil (antihypertensive), Raltegravir (HIV integrase) and Zibotentan (anti-cancer agent) agent (Fig. 1) (Sharma et al. 2010; Lotfi et al. 2010; El-Sayed et al. 2012). Table 2

Schiff bases and its derivatives with their azomethine (imines) functional group exhibited a wide range of therapeutic profile owing to its interesting bioactivity. Additionally, Schiff bases that contained heterocyclic derivatives were reported to possess the broad spectrum of biological and therapeutic potentials including antimicrobial (Prakash et al., 2013), anti-helminthic (Revanasiddappa et al., 2013), antiviral (Kumar et al., 2010) and antitumor agents (Fig. 2) (Zhou et al., 2007).

Keeping in view, the biological significance of pyridine (El-Naggar et al. 2018, Boraei et al. 2021) and oxadiazole-schiff base (Sardar et al., 2022; Ullah et al. 2020) analogs, herein this study we have designed and synthesized novel scaffolds of pyridine-derived bis-oxadiazole bearing bis-schiff base as potential inhibitors of thymidine phosphorylase in search of lead molecules (Fig. 3).

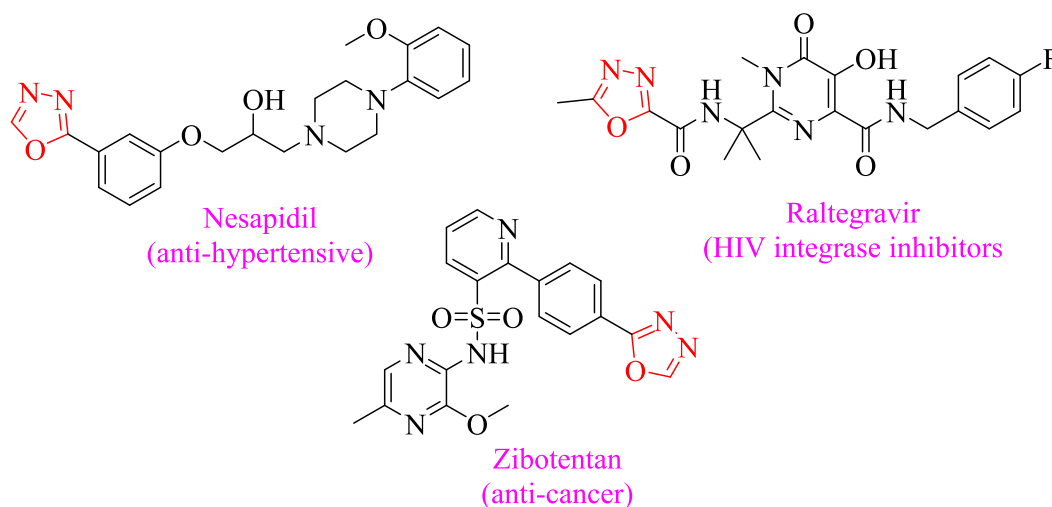


**Fig. 1** Biologically active drugs bearing 1,3,4-oxadiazole skeleton.

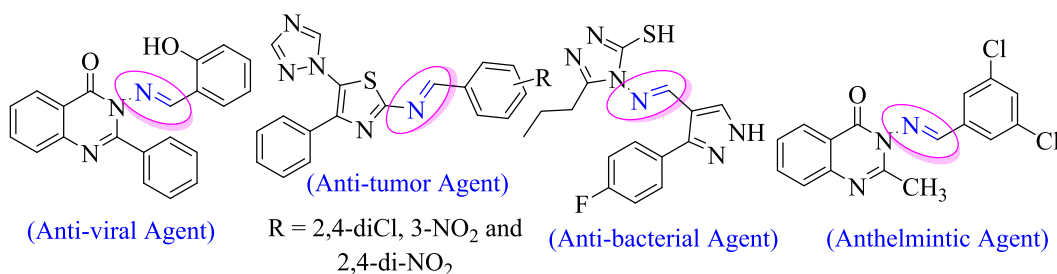


**Fig. 2** Biological profile of schiff base containing heterocyclic compounds.

## 2. Experimental

### 2.1. General information

Sigma-Aldrich was source from which the analytical-grade solvents and reagents, which were then applied without further purification. An FTS 3000 MX, Bio-RAD Merlin (Excalibur Model) spectrophotometer was used to run IR spectra on KBr discs. On the MAT 113D and MAT 312 mass spectrometers, electron impact (EI) was used to record mass spectra. The <sup>1</sup>H and <sup>13</sup>C NMR spectra on Advance Bruker (AM) spectrometers operating at 600 and 150 MHz were recorded. The coupling constants (J) are given in Hz, and the chemical shift values are given in ppm, relative to tetramethylsilane (TMS) as an internal reference. Singlet (s), doublet (d), triplet (t), doublet of doublets (dd), doublet of triplets (dt), quartet (q), or multiplet are the terms used to describe multiples (m). Aluminum plates with precoated silica gel were used for the thin-layer chromatography (TLC) procedure (Kieselgel 60, 254, E. Merck, Germany). TLC chromatograms were seen at 254 and 366 nm in ultraviolet light. On Stuart SMP10 melting point equipment, the melting points of compounds were evaluated.

### 2.2. General procedure for the synthesis of pyridine-derived bis-oxadiazole bearing bis-schiff base derivatives (4a-l)

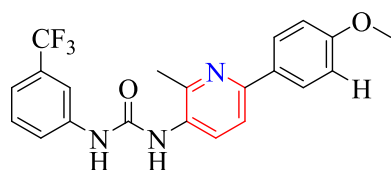
The synthesis of pyridine-derived bis-oxadiazole bearing bis-schiff bases (**4a-l**) were completed in three steps: In first step,

pyridine-based bis-semicarbazone substrate (**2**) was synthesized by adding semicarbazide (2 equivalent) to stirred solution of pyridine-2,6-dicarboxaldehyde (**1**) (1 equivalent) in methanol (10 mL) along with few drops of acetic acid (catalyst). Upon completion, solvent was evaporated and resulting solid residue (1 equivalent) was further subjected to an oxidative cyclization with molecular iodine (2 equivalent) and potassium carbonate (1.8 mmol) in 1,4-dioxane (10 mL) to deliver pyridine-based bis-oxadiazole (**3**). In the last step, pyridine-based bis-oxadiazole substrate (**3**) (1 equivalent) was reacted with different substituted benzaldehyde (2 equivalent) in methanol (10 mL) under catalytic amount of acetic acid to afford the targeted pyridine-based bis-oxadiazole bearing bis-schiff base derivatives (scheme 1)(**4a-l**) in appropriate yield.

## 3. Result and discussion

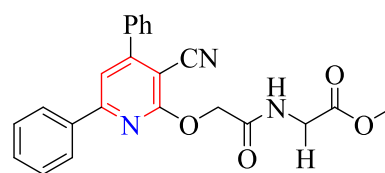
### 3.1. Chemistry

In this study, novel scaffolds of pyridine-derived bis-oxadiazole bearing bis-schiff base analogs (**4a-l**) were afforded through several steps. In the first step, pyridine-2,6-dicarbaldehyde (**1**) was reacted with two molar semicarbazide solution being stirred in methanol and few drops of acetic acid (catalyst) and mixture was put on reflux for 4 hrs to obtain an intermediate (**2**) which further underwent an oxidative cyclization with K<sub>2</sub>CO<sub>3</sub> and I<sub>2</sub> in 1,4-dioxane to yield pyridine-derived bis-oxadiazole substrate (**3**). Finally, an intermediate

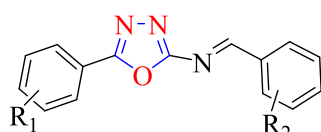
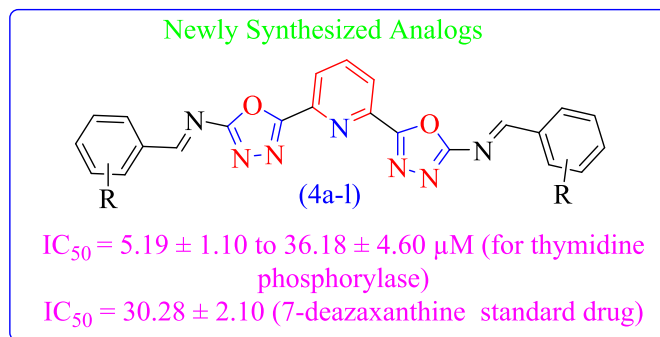


(El-Naggar, et al. 2018)

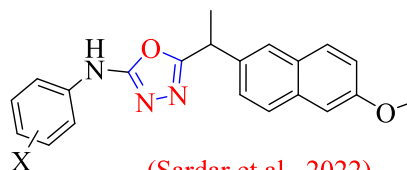
$IC_{50} = 5.0 \pm 1.91 \mu M$  (anti-proliferative activity)  $IC_{50} = 13.9 \pm 0.98 \mu M$  (for cytotoxic activity against HepG2 (liver cell line))  
 $IC_{50} = 0.09 \pm 0.01 \mu M$  ( Sorafenib standard drug)



(Boraci, et al. 2021)



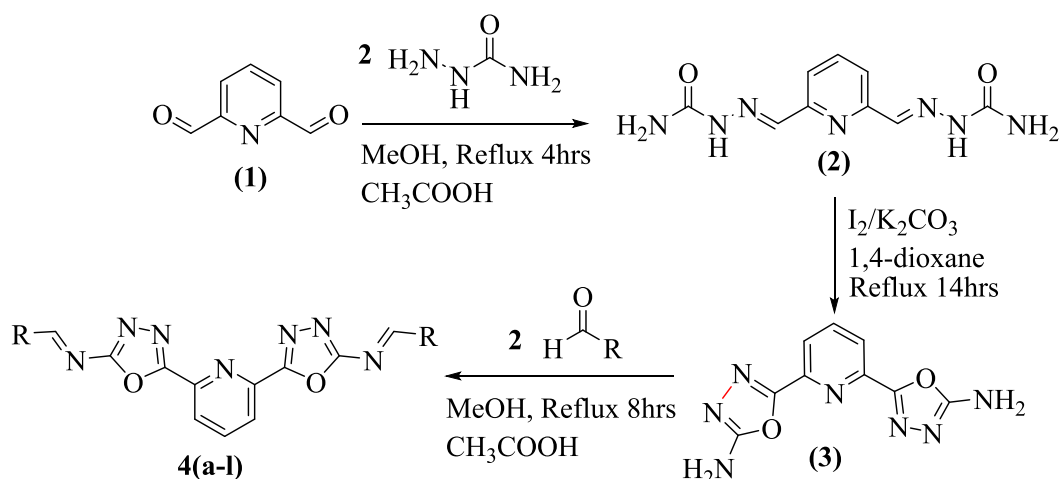
(Ullah, et al. 2020)



(Sardar et al., 2022)

$IC_{50} = 0.30 \pm 0.2$  to  $35.1 \pm 0.80 \mu M$  (for  $\alpha$ -glucosidase)  $IC_{50} = 1.1 \pm 1.17$  to  $96.9 \pm 1.11 \mu M$  (for  $\alpha$ -glucosidase)  
 $IC_{50} = 38.45 \pm 0.80 \mu M$  (standard acarbose)  $IC_{50} = 375.82 \pm 1.76 \mu M$  (standard acarbose)

Fig. 3 Rational of the current study.



Scheme 1 Synthesis of pyridine-derived bis-oxadiazole bearing bis-schiff base derivatives.

(3) was further refluxed and stirred with two moles of different substituted benzaldehyde in MeOH along with catalytic amount of glacial acetic acid. The residue was heated for

8hrs over pre-heated sand bath to afford targeted pyridine-derived bis-oxadiazole bearing bis-schiff base derivatives (4a-1). As the reaction was completed, the solvent was

evaporated to form solid form of targeted compounds which were washed, recrystallized and dried to access the purified form of pyridine-derived bis-oxadiazole bearing bis-schiff base derivatives (**4a-l**). The precise structures of the synthesized compounds were elucidated using various spectroscopic tools including  $^1\text{NMR}$ ,  $^{13}\text{CNMR}$  and HR-EIMS (scheme 1). The  $^1\text{H NMR}$  spectrum of analog **4d** was recorded in DMSO  $d_6$  on a Bruker operating at 600 MHz. The most downfield singlet was observed for (HC=N) proton resonating at chemical shift of  $\delta_{\text{H}}$  10.27 ppm. One more singlet was also observed for three methyl protons resonating at chemical shift values of  $\delta_{\text{H}}$  5.38. The molecule comprises of two symmetrical benzene rings bearing 2-methyl and 4-chloro substitutions and pyridine ring containing 3-protons attached to each rings. Among pyridine ring protons, a doublet was appeared for two chemically equivalent protons resonating at chemical shift values of  $\delta_{\text{H}}$  7.88 ppm with coupling constant of 8.4 Hz, while third proton of pyridine ring also resonated as doublet with chemical shift value appearing at  $\delta_{\text{H}}$  7.64 along with coupling constant value of 6.8 Hz. For symmetrical benzene rings, we might expect the proton NMR spectrum only for one half of the molecules. The proton present at 3-position of extended benzene ring coupled to its neighboring *meta*-proton and appeared as doublet with chemical shift values of  $\delta_{\text{H}}$  7.84 along with coupling constant value of 1.8 Hz, indicating that *meta*-coupling take place. However, the two protons present at 5- and 6-position of benzene ring coupled to one another to give two different doublet appearing at chemical shift values of  $\delta_{\text{H}}$  7.72 ( $J = 8.4$  Hz) and  $\delta_{\text{H}}$  7.37 ( $J = 6.6$  Hz) respectively.

### 3.2. In vitro thymidine phosphorylase inhibitory activity (4a-l)

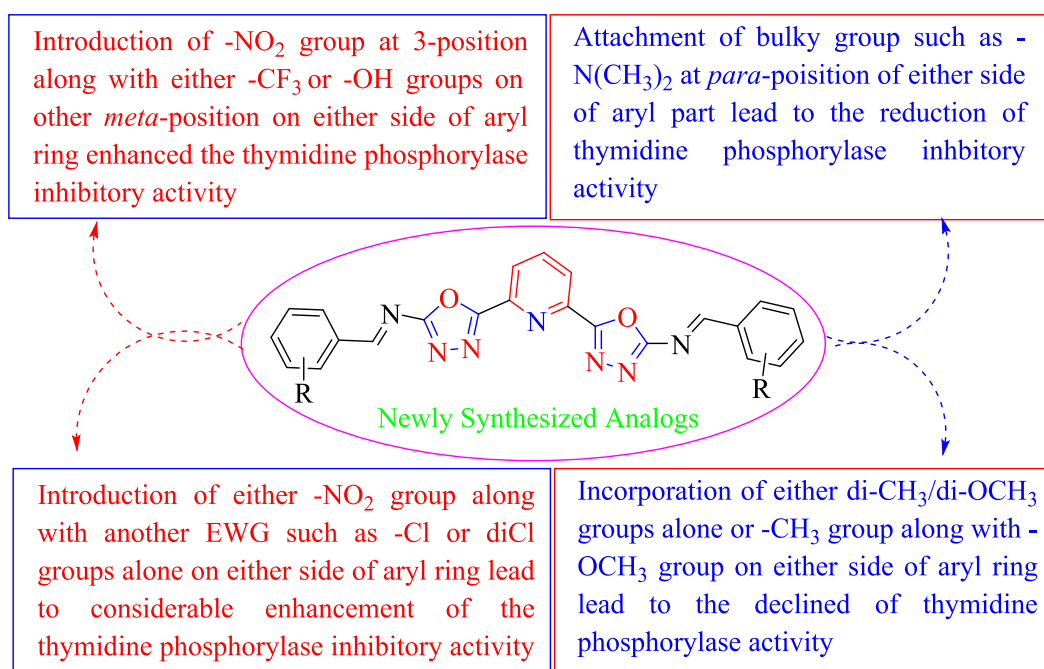
#### 3.2.1. Structure-activity relationship (SAR) for thymidine phosphorylase activity

In this study, twelve analogs of pyridine-derived bis-oxadiazole bearing bis-schiff base derivatives were afforded and then

assessed for their in vitro thymidine phosphorylase inhibitory activity based on literature known protocol under the positive control of 7-deazaxanthine<sup>b</sup>. Based on substitution(s) pattern around aryl part, the SAR studies was carried out for all synthesized analogs. It seemed from SAR studies that all parts including pyridine, bis-oxadiazole, bis-schiff base, both aryl parts and substitution(s) around aryl parts are actively contributing in the inhibitory potentials of thymidine phosphorylase (Fig. 4).

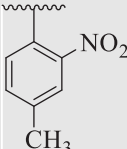
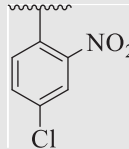
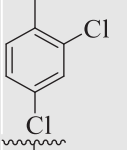
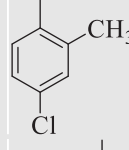
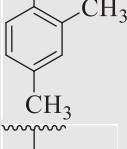
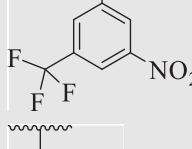
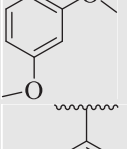
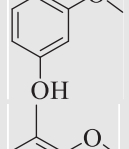
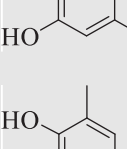
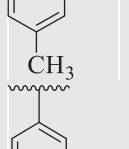
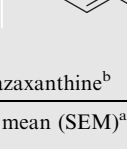
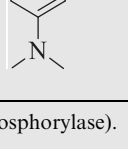
Analog **4f** bearing 3-trifluoro-5-nitro on aromatic-aryl moiety was recognized as most active scaffolds of thymidine phosphorylase enzyme and showed potency many folds better than standard 7-deazaxanthine. Similarly, analog **4i** bearing 3-hydroxy-5-nitro groups at aryl part also displayed much folds better inhibitory potential than standard 7-deazaxanthine drug. These **4f** and **4i** scaffolds were recorded as the most potent inhibitors of thymidine phosphorylase enzyme among the current synthesized series. The elevation in the inhibitory potentials of these analogs was due to attached electron withdrawing  $-\text{NO}_2$ ,  $-\text{CF}_3$  and  $-\text{OH}$  groups which interacts with thymidine phosphorylase active site via strong intermolecular force of attraction such as hydrogen bonding and halogen fluorine interactions and hence enhance the inhibitory potentials. By comparing analog **4f** which holds  $-\text{CF}_3$  group instead of  $-\text{OH}$  group at one of the *meta*-position of aryl part of **4i** analog, the analog **4f** displayed better activity than **4i** analog due to stronger interactions offered by  $-\text{CF}_3$  group than  $-\text{OH}$  group as in the case of analog **4i** (Table 1). However, the analog **4i** displayed better potency when compared to its structurally similar analog **4k** (bearing 2-hydroxy-5-nitro) showing that difference in substituent(s) position around the aryl part resulted to different inhibitory potentials (Table 1).Table 2. Table 2.

The analog **4c** bearing di-chloro moieties at 2,4-position of aryl part was found to be encouraging for inhibition of thymidine phosphorylase enzyme and displayed 2-folds more



**Fig. 4** Summary of SAR studies of synthesized pyridine-derived bis-oxadiazole-based bis-schiff base derivatives.

**Table 1** Different substituent(s) and in vitro thymidine phosphorylase inhibitory activity of pyridine-derived bis-oxadiazole bearing bis-schiff base derivatives (**4a-l**).

S.NO	R	IC <sub>50</sub> ± SEM <sup>a</sup> [μM]	S.NO	R	IC <sub>50</sub> ± SEM <sup>a</sup> [μM]
<b>4a</b>		19.73 ± 2.30	<b>4b</b>		16.14 ± 1.20
<b>4c</b>		18.93 ± 1.60	<b>4d</b>		22.78 ± 1.80
<b>4e</b>		30.47 ± 3.70	<b>4f</b>		5.19 ± 1.10
<b>4g</b>		23.13 ± 1.90	<b>4h</b>		21.56 ± 2.50
<b>4i</b>		5.88 ± 1.10	<b>4j</b>		26.63 ± 2.90
<b>4k</b>		6.67 ± 1.10	<b>4l</b>		36.18 ± 4.60
Standard 7-Deazaxanthine <sup>b</sup>					30.28 ± 2.10 μM

Standard error mean (SEM)<sup>a</sup> and 7-Deazaxanthine<sup>b</sup> (standard inhibitor for thymidine phosphorylase).

potency than standard 7-deazaxanthine drug. However, the inhibitory potentials was further increased by replacing *ortho*-Cl group of analog **4c** with -NO<sub>2</sub> group as in analog **4b** bearing 2-NO<sub>2</sub>-4-Cl moieties at aryl part. This enhanced activity of analog **4b** was due to stronger EW effect of -NO<sub>2</sub> group. In addition, the inhibitory potential of analog **4c** was declined by replacing *ortho*-Cl moiety with -CH<sub>3</sub> group as in case of analog **4d** (bearing *ortho*-CH<sub>3</sub> and *para*-Cl moieties) (Table 1).

By comparing analog **4e** bearing diCH<sub>3</sub> moieties at 2,4-position of aryl ring with analog **4g** bearing diOCH<sub>3</sub> groups at 2,4-position of aryl ring, the analog **4g** showed better activity than analog **4e**. This enhanced activity of analog **4g** was due to interactions of lone pair of electrons of oxygen of methoxy group with benzene ring which further regain its stability on interactions with the active sites of thymidine phosphorylase and therefore enhanced the inhibitory potential. The inhibitory potential of analog **4g** was further increased by replacing *para*-methoxy with *para*-hydroxy group as in case of analog **4h**. This was due to interaction of hydroxy group through hydrogen bonding with the active site of thymidine phosphorylase (Table 1). The analog **4i** bearing dimethylamino at 4-position

of aryl part was identified as least inhibitor of thymidine phosphorylase among the current synthesized series and displayed less potency than standard 7-deazaxanthine. This less potency of analog **4i** was due to incapable of interaction offered by dimethylamino with the active site of thymidine phosphorylase enzyme because two bulky methyl groups attached with nitrogen which not allowing the lone pair of nitrogen to interact with the benzene ring (Table 1).

Overall, it was concluded that the inhibitory potential of synthesized analogs was greatly affected by alteration in EW/ED nature, position and number/s of attached substituent(s) around aryl part.

### 3.3. Molecular docking study

The synthesized scaffolds and their inhibitory profile against the thymidine phosphorylase enzyme are listed in Table 1. It was found that the position, type, and number of functional moieties connected to the aryl portion of pyridine-derived bis-oxadiazole carrying bis-schiff base skeleton were substantially correlated with the IC<sub>50</sub> values of thymidine phosphory-

**Table 2** The different types of interactions between active analogs (**4f**, **4i** and **4k**) as well as standard 7-deazaxanthine drug and interactive residues of amino acids of targeted thymidine phosphorylase with binding affinities.

Active analogs	Targeted enzyme	Receptors	Types of interaction	Binding affinities Kcal/mol
4f	Thymidine phosphorylase	PHE-206, ARG-91, TYR-205 and HIS-94 ARG-600, THR-599, THR-204, VAL-96 and PHE-200 ASP-207 VAL-96 and PHE-200 VAL-201	Halogen (fluorine) HB  Pi-Anion Pi-Pi stacked Pi-alkyl	-10.23
4i	Thymidine phosphorylase	ARG-600, THR-599, SER-597 and THR-204 GLN-202 VAL-96 and PHE-200 VAL-201	HB Pi-donor HB Pi-alkyl Pi-sigma and Alkyl Pi-Anion	-9.89
4f	Thymidine phosphorylase	ASP-207 and GLU-597 GLN-902, ARG-56, ARG48 and ARG57 ARG-91 and PHE-51 VAL-96 PHE-51	HB Pi-Pi T shaped Pi-alkyl Pi-alkyl	-7.37
7-Deazaxanthine	Thymidine phosphorylase	GLY-145, HIS-116, THR-151 SER-117 HIS-116	HB Pi-donor HB Pi-Pi T shaped	-5.67

lase inhibitors. Molecular docking was used to explore the position, kind, and quantity of attached substituents as well as enzymatic inhibition, as well as to further develop the binding contacts of newly provided scaffolds with active residues of both targeted thymidine phosphorylase enzymes. The detailed PLI analysis of the most potent analogs such as **4f**, **4i** and **4k** against thymidine phosphorylase revealed that they had established a number of significant interactions with the active residues of targeted thymidine phosphorylase enzyme. These interactions may have improved the inhibitory profile of these active analogs against the targeted thymidine phosphorylase. During docking the scoring function of grid box and their coordinate's configuration were set (center\_x = 21.807, center\_y = 17.01 and center\_z = 42.393 and size for x, y and z = 40 as well as the exhaustiveness = 8). There were 9 different poses have been generated for each ligand and the remarkable pose was found with least energy. In this regard scaffold-4f exhibited different energy poses (pose-1 having -10.23). Similarly the remaining poses of the ligand showed different binding affinities (-8, -7, -7, -6, -5, -5, -5 and -4). The most active scaffold **4f** established several key interactions with the active site of thymidine phosphorylase enzyme including Phe206 (halogen (fluorine), Tyr205 (halogen (fluorine), Arg600 (CHB), Ser597 (CHB), Thr599 (CHB), Thr204 (CHB), Asp207 (pi-anion), Arg91 ((halogen (fluorine), His94 (halogen (fluorine), Val96 (CHB & pi-pi stacking), Phe200 (CHB & pi-pi stacking) and Val201 (pi-alkyl) interactions. Due to the -NO<sub>2</sub> and -CF<sub>3</sub> (electron withdrawing) groups attached to the aryl part, which largely remove the electronic density from the Ph-ring and make it more susceptible to interactions with the active site of the thymidine phosphorylase enzyme, and hence analog **4f** increased the inhibitory potentials against the thymidine phosphorylase enzyme (Fig. 5).

Likewise, scaffold 4i was also found with better binding affinities (there nine different poses having -9.89 to -6 binding affinity). Similar to this, the second-most active analogue **4i** protein-ligand interaction (PLI) profile against the thymidine

phosphorylase enzyme showed a number of significant contacts with the enzyme's active site, including residues Arg600 (CHB), Thr599 (CHB), Ser597 (CHB), Asp207 (pi-anion), Thr204 (CHB), Glu597 (pi-anion), Val201 (pi-sigma & alkyl), Val96 & Phe200 (pi-alkyl) and Gln202 (pi-donor HB) interactions (Fig. 6).

Scaffold 4k was also found with better binding affinities (there nine different poses having -7.37 to -4 binding affinity). The third-most active scaffold **4k** protein-ligand interaction (PLI) profile found that this analog displayed a number of strong interactions with the active region of the thymidine phosphorylase enzyme, including Val96 (pi-alkyl), Gln902 (CHB), Arg91 (pi-pi T shaped), Phe51 (pi-alkyl & pi-pi T shaped), Arg56 (CHB), Arg57 (CHB), Arg48 (CHB) and Van der Waals interactions (Fig. 7).

By comparing the protein-ligand interactions (PLI) profile of the most active scaffolds **4f**, **4i** and **4k** with standard 7-deazaxanthine drug, the most active analogs furnished some additional interactions including pi-alkyl, pi-anion, pi-sigma, pi-pi stacked and alkyl interactions in addition to that developed by standard 7-deazaxanthine with the active sites of targeted thymidine phosphorylase enzymes than standard 7-deazaxanthine which established only hydrogen bond, pi-donor hydrogen bond, carbon hydrogen bond and pi-pi T shaped interactions (Fig. 8).

### 3.4. ADMET prediction

ADMET prediction represents the property of Absorption, Distribution, Metabolism, Excretion, and Toxicity. In this study various factor regarding to drug like properties have been studied. Here in this study analog-4f, 4i and 4k were found with most effective properties such as logP = -6.98 c m/s, Lipinski violations = 2, Ghose violations = 3, veber violation = 2, Egan violation = 2, Muegge violation = 3, Bioavailability score = 0.17, pain alert = 0 Brenk alerts = 3 etc.



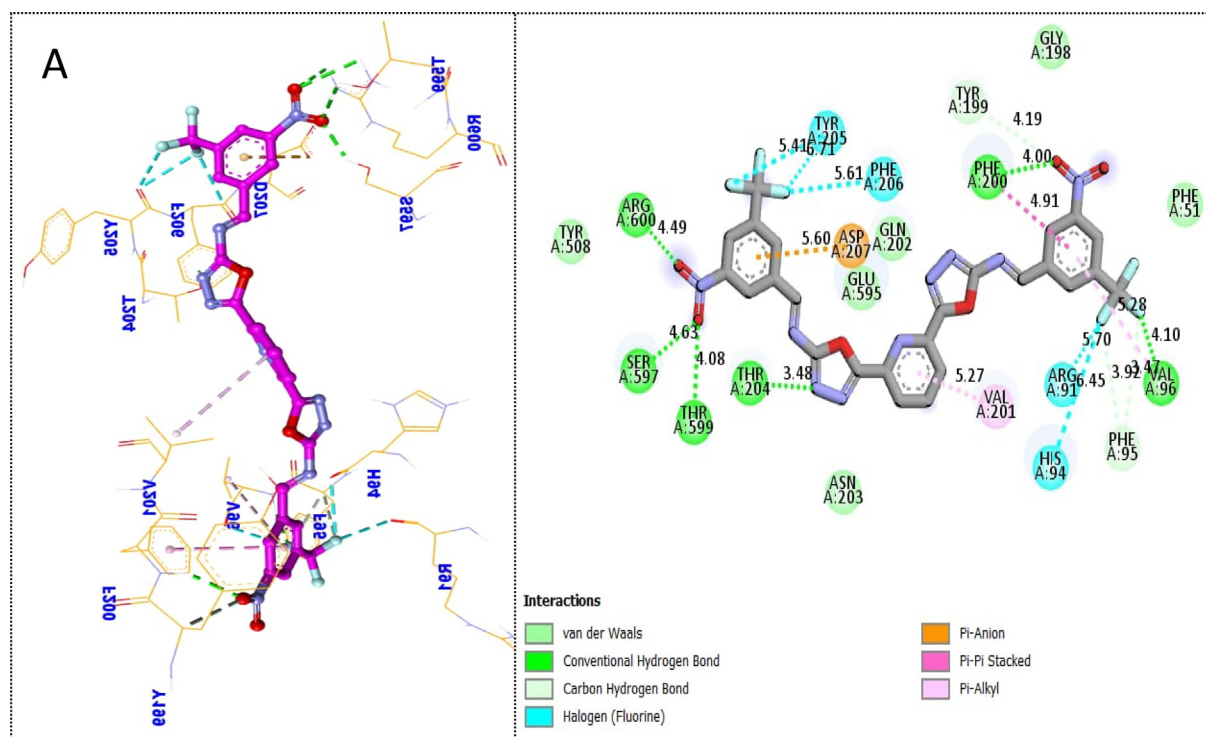


**Fig. 5** Protein-ligand interaction profile (PLI) of most active scaffold **4f** (**A**) against targeted thymidine phosphorylase and its 3D (left) and 2D (right) diagram.

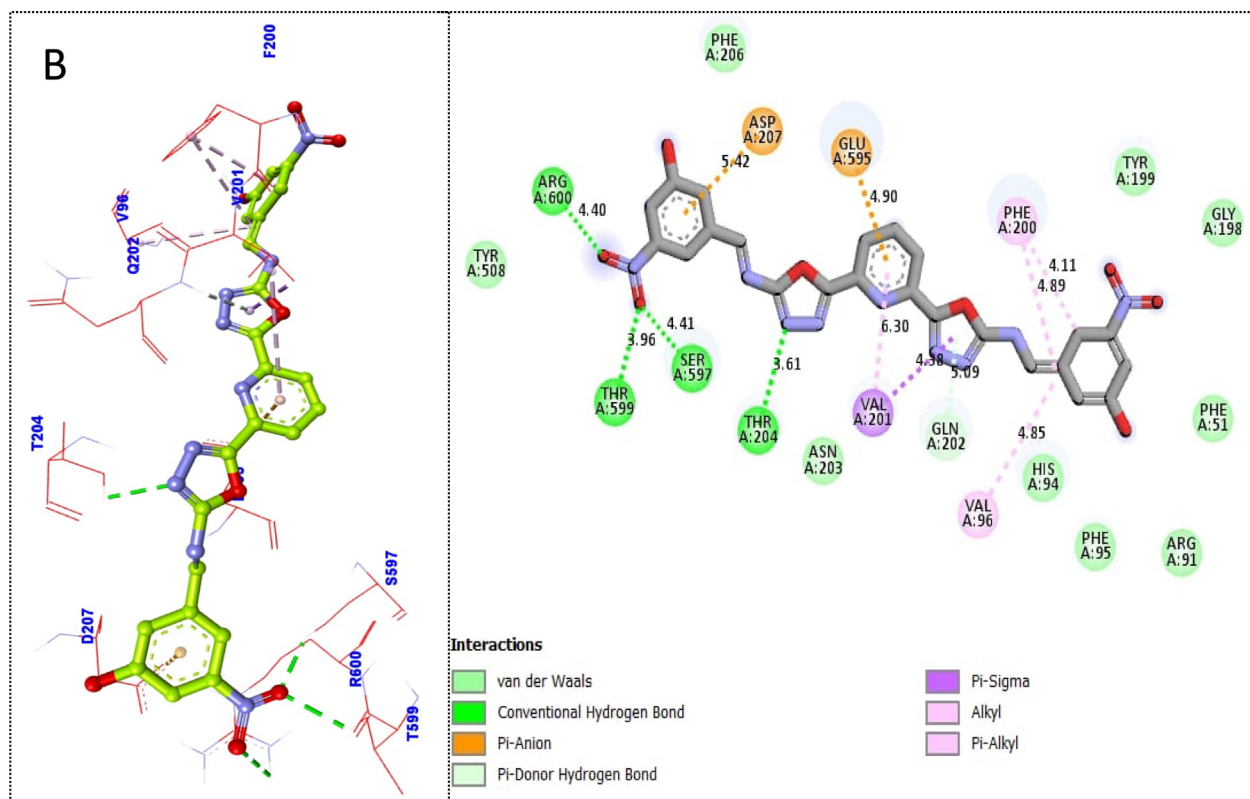


**Fig. 6** Protein-ligand interaction profile (PLI) of 2nd most active scaffold **4i** (**B**) against targeted thymidine phosphorylase and its 3D (left) and 2D (right) diagram.

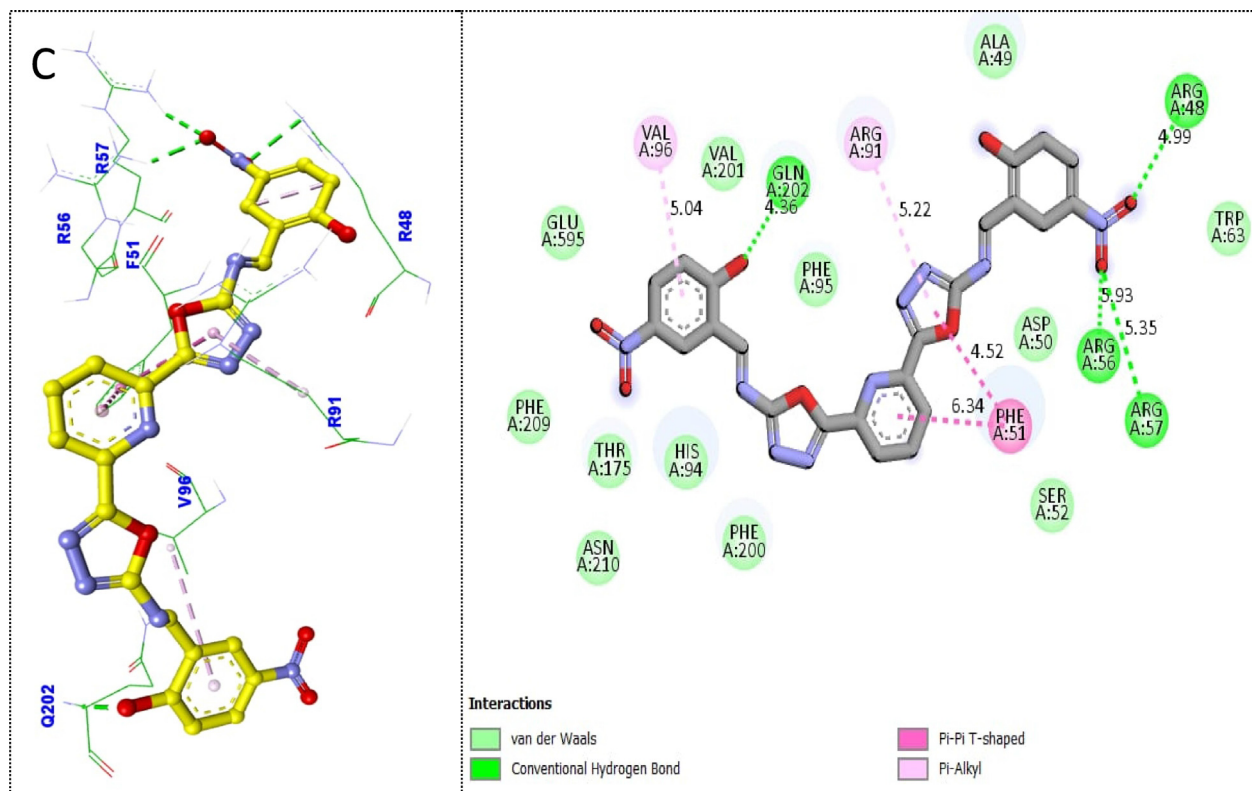


**Fig. 7** Protein-ligand interaction profile (PLI) of 3rd most active analog **4 k(C)** against targeted thymidine phosphorylase and its 3D (left) and 2D (right) diagram.

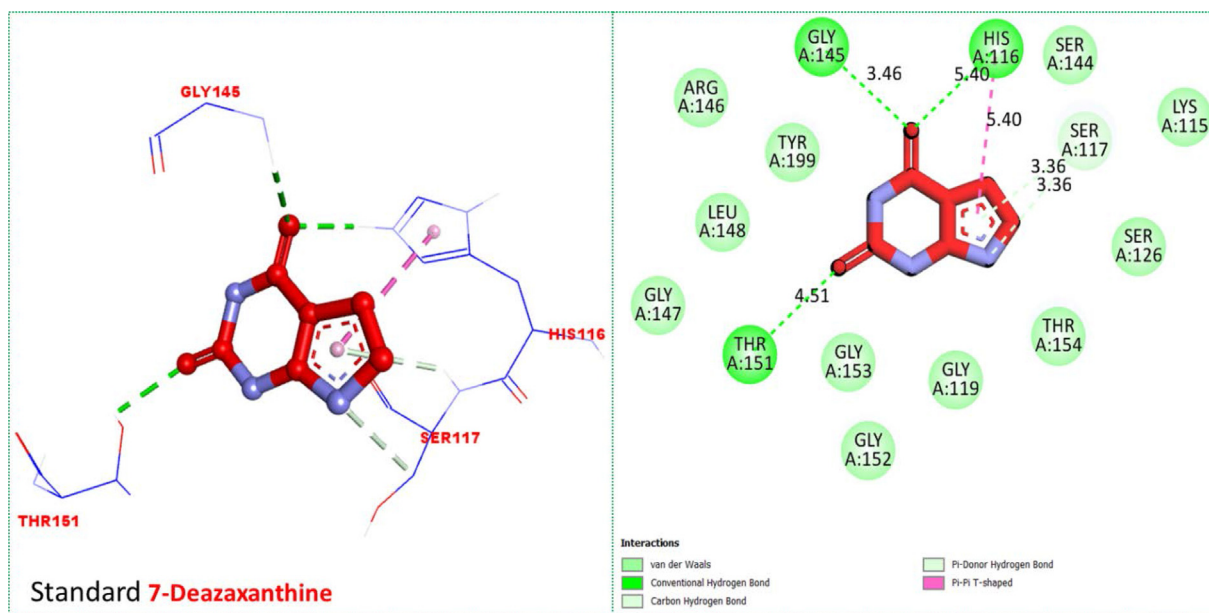


**Fig. 8** Protein-ligand interaction profile (PLI) of standard 7-Deazaxanthine against targeted thymidine phosphorylase and its 3D (left) and 2D (right) diagram.

#### 4. Conclusion

In conclusion, we have reported a facile protocol for the synthesis of a library of bis-oxadiazole-based bis-schiff base derivatives (**4a-l**) containing pyridine moiety via iodine-mediated oxidative cyclization of pyridine-based semicarbazone substrate followed by reacted to different substituted benzaldehyde. The entire synthesized scaffolds (**4a-l**) were evaluated for their in vitro thymidine phosphorylase inhibition profile and further structurally elucidated using various spectroscopic tools including NMR and HREIMS. All compounds were identified to have significant to moderate thymidine phosphorylase inhibitory activity with  $IC_{50}$  values ranging from  $5.19 \pm 1.10$  to  $36.18 \pm 4.60$   $\mu$ M, when compared to 7-deazaxanthine ( $IC_{50} = 30.28 \pm 2.10$   $\mu$ M) as reference drug. The most active thymidine phosphorylase inhibitory compounds were **4f**, **4i** and **4k**, which also represented the lowest  $IC_{50}$  values with relative potency many folds better than reference drug. Apart from these, the SAR studies were carried out for all analogs based on substitution(s) pattern around aryl part attached to pyridine-derived bis-oxadiazole bearing bis-schiff base. The screening results and the SAR studies suggested that the electron withdrawing groups and their positions played an important role in the inhibitory potential. Docking studies with in the thymidine phosphorylase active sites revealed that compounds **4f**, **4i** and **4k** showed binding orientation fit well into the active sites of target and adopted several key interactions with catalytic cavity of targeted enzyme. The oxadiazole moiety was also found to form important interaction with the amino acid residues lining the active site gorge of thymidine phosphorylase. The results suggest that new bis-oxadiazole-based bis-schiff base derivatives containing pyridine moiety, especially **4f**, **4i** and **4k** may serve as new lead molecules for development of new and improved bis-oxadiazole-based bis-schiff base inhibitors.

#### CRedit authorship contribution statement

**Rafaqat Hussain:** Methodology. **Wajid Rehman:** Conceptualization, Writing – original draft, Supervision, Project administration, Writing – original draft, Writing – review & editing. **Fazal Rahim:** Conceptualization. **Shoaib Khan:** Software, Visualization. **Ashwag S. Alanazi:** Validation, Funding acquisition. **Mohammed M. Alanazi:** Resources, Writing – review & editing. **Liaqat Rasheed:** Investigation. **Yousaf Khan:** Data curation. **Syed Adnan. Ali. Shah:** Formal analysis. **Muhammad Taha:** .

#### Declaration of Competing Interest

The authors declare that they have no known competing financial interests or personal relationships that could have appeared to influence the work reported in this paper.

#### Acknowledgements

The authors extend their appreciation to the Researchers Supporting Project number (RSPD2023R628), King Saud University, Riyadh, Saudi Arabia for supporting this research.

The authors also extend their appreciation to Princess Nourah bint Abdulrahman University Researchers Supporting Project number (PNURSP2023R342), Princess Nourah bint Abdulrahman University, Riyadh, Saudi Arabia for supporting this research.

#### Appendix A. Supplementary material

[2.3. Spectral Analysis; 2.4 Assay protocol for docking study and 2.5 Assay protocol for thymidine phosphorylase inhibition were provided in supplementary information]. Supplementary data to this article can be found online at <https://doi.org/10.1016/j.arabjc.2023.104773>.

#### References

- Asai, K. et al, 1992. Neurotrophic action of gliostatin on cortical neurons. Identity of gliostatin and platelet-derived endothelial cell growth factor. *J. Biol. Chem.* 267 (28), 20311–20316.
- Bijnsdorp, I. et al, 2011. Thymidine phosphorylase in cancer cells stimulates human endothelial cell migration and invasion by the secretion of angiogenic factors. *Br. J. Cancer* 104 (7), 1185–1192.
- Boraei, A.T. et al, 2021. Synthesis of new substituted pyridine derivatives as potent anti-liver cancer agents through apoptosis induction: In vitro, in vivo, and in silico integrated approaches. *Bioorg. Chem.* 111, 104877.
- Brown, N.S. et al, 2000. Thymidine phosphorylase induces carcinoma cell oxidative stress and promotes secretion of angiogenic factors. *Cancer Res.* 60 (22), 6298–6302.
- de Moura Sperotto, N.D. et al, 2019. Design of novel inhibitors of human thymidine phosphorylase: synthesis, enzyme inhibition, in vitro toxicity, and impact on human glioblastoma cancer. *J. Med. Chem.* 62 (3), 1231–1245.
- Dogan, H.N. et al, 2002. Synthesis of new 2, 5-disubstituted-1, 3, 4-thiadiazoles and preliminary evaluation of anticonvulsant and antimicrobial activities. *Bioorg. Med. Chem.* 10 (9), 2893–2898.
- Du, L.-H., Luo, X.-P., 2010. Efficient one-pot synthesis of benzimidazoles under solvent-free conditions. *Synthetic Commun.* 40 (19), 2880–2886.
- El-Emam, A.A. et al, 2004. Synthesis, antimicrobial, and anti-HIV-1 activity of certain 5-(1-adamantyl)-2-substituted thio-1, 3, 4-oxadiazoles and 5-(1-adamantyl)-3-substituted aminomethyl-1, 3, 4-oxadiazole-2-thiones. *Bioorg. Med. Chem.* 12 (19), 5107–5113.
- El-Naggar, M. et al, 2018. Pyridine-ureas as potential anticancer agents: synthesis and in vitro biological evaluation. *Molecules* 23 (6), 1459.
- El-Sayed, W.A. et al, 2012. Synthesis and antimicrobial activity of new 2,5-disubstituted 1,3,4-oxadiazoles and 1,2,4-triazoles and their sugar derivatives. *Chin. J. Chem.* 30, 77–83.
- Friedkin, M., Roberts, D., 1954. The enzymatic synthesis of nucleosides: I. Thymidine phosphorylase in mammalian tissue. *J. Biol. Chem.* 207 (1), 245–256.
- Haraguchi, M. et al, 1994. Angiogenic activity of enzymes. *Nature* 368 (6468), 198.
- Hotchkiss, K.A. et al, 2003. Mechanisms by which tumor cells and monocytes expressing the angiogenic factor thymidine phosphorylase mediate human endothelial cell migration. *Cancer Res.* 63 (2), 527–533.
- Husain, A. et al, 2009. Fenbufen based 3-[5-(substituted aryl)-1, 3, 4-oxadiazol-2-yl]-1-(biphenyl-4-yl) propan-1-ones as safer antiinflammatory and analgesic agents. *Eur. J. Med. Chem.* 44 (9), 3798–3804.
- Ikeda, R. et al, 2002. Molecular basis for the inhibition of hypoxia-induced apoptosis by 2-deoxy-D-ribose. *Biochem. Biophys. Res. Commun.* 291 (4), 806–812.
- Ikeda, R. et al, 2003. Thymidine phosphorylase inhibits apoptosis induced by cisplatin. *Biochem. Biophys. Res. Commun.* 301 (2), 358–363.
- Iltzsch, M.H. et al, 1985. Kinetic studies of thymidine phosphorylase from mouse liver. *Biochemistry* 24 (24), 6799–6807.

- Jeung, H.-C. et al, 2005. Thymidine phosphorylase suppresses apoptosis induced by microtubule-interfering agents. *Biochem. Pharmacol.* 70 (1), 13–21.
- Jeung, H.-C. et al, 2006. Protection against DNA damage-induced apoptosis by the angiogenic factor thymidine phosphorylase. *FEBS Lett.* 580 (5), 1294–1302.
- Katritzky, A.R. et al, 2010. *Handbook of heterocyclic chemistry.* Elsevier.
- Kumar, K.S., Ganguly, S., Veerasamy, R., De Clercq, E., 2010. Synthesis, antiviral activity and cytotoxicity evaluation of Schiff bases of some 2-phenyl quinazoline-4 (3) H-ones. *Eur. J. Med. Chem.* 45 (11), 5474–5479.
- Leung, D. et al, 2005. Discovery of an exceptionally potent and selective class of fatty acid amide hydrolase inhibitors enlisting proteome-wide selectivity screening: concurrent optimization of enzyme inhibitor potency and selectivity. *Bioorg. Med. Chem. Lett.* 15 (5), 1423–1428.
- Liekens, S. et al, 2002. Anti-angiogenic activity of a novel multi-substrate analogue inhibitor of thymidine phosphorylase. *FEBS Lett.* 510 (1–2), 83–88.
- Lotfi, B. et al, 2010. Electrocyclization of semicarbazone; A novel route of green synthesis of 2,5-disubstituted-1,3,4-oxadiazoles. *Int. J. Electrochem. Sci.* 6, 1991–2000.
- Matsuura, T. et al, 1999. Thymidine phosphorylase expression is associated with both increase of intratumoral microvessels and decrease of apoptosis in human colorectal carcinomas. *Cancer Res.* 59 (19), 5037–5040.
- Miyadera, K. et al, 1995. Role of thymidine phosphorylase activity in the angiogenic effect of platelet-derived endothelial cell growth factor/thymidine phosphorylase. *Cancer Res.* 55 (8), 1687–1690.
- Moghaddam, A., Bicknell, R., 1992. Expression of platelet-derived endothelial cell growth factor in *Escherichia coli* and confirmation of its thymidine phosphorylase activity. *Biochemistry* 31 (48), 12141–12146.
- Moghaddam, A., et al. (1995). “Thymidine phosphorylase is angiogenic and promotes tumor growth. *Proc. Natl. Acad. Sci.* 92(4): 998–1002.
- Omar, F.A. et al, 1996. Design, synthesis and antiinflammatory activity of some 1, 3, 4-oxadiazole derivatives. *Eur. J. Med. Chem.* 31 (10), 819–825.
- O’Neal, J. et al, 1962. Potential hypoglycemic agents: 1, 3, 4-Oxadiazoles and related compounds. *J. Med. Chem.* 5 (3), 617–626.
- Orlek, B.S. et al, 1991. Comparison of azabicyclic esters and oxadiazoles as ligands for the muscarinic receptor. *J. Med. Chem.* 34 (9), 2726–2735.
- Palaska, E. et al, 2002. Synthesis and anti-inflammatory activity of 1-acylthiosemicarbazides, 1, 3, 4-oxadiazoles, 1, 3, 4-thiadiazoles and 1, 2, 4-triazole-3-thiones. *Il Farmaco* 57 (2), 101–107.
- Pattan, S. R., et al., 2009. Synthesis and evaluation of some novel substituted 1, 3, 4-oxadiazole and pyrazole derivatives for antitubercular activity.
- Prakash, C.R., Raja, S., 2013. Synthesis, characterization and in vitro antimicrobial activity of some novel 5-substituted Schiff and Mannich base of isatin derivatives. *J. Saudi Chem. Soc.* 17 (3), 337–344.
- Revanasiddappa, H.D., Prasad, K.S., Kumar, L.S., Jayalakshmi, B., 2010. Synthesis and biological activity of new Schiff bases containing 4 (3H)-quinazolinone ring system. *Int. J. ChemTech Res.* 2 (2), 1344–1349.
- Salar, U. et al, 2015. Biology-Oriented Syntheses (BIOS) of Novel Santonic-1, 3, 4-oxadiazole Derivatives under Microwave-Irradiation and their Antimicrobial Activity. *J. Chem. Soc. Pak.* 37 (5).
- Sardar, A. et al, 2022. Design, synthesis, in vitro and in silico studies of naproxen derivatives as dual lipoxygenase and  $\alpha$ -glucosidase inhibitors. *J. Saudi Chem. Soc.* 26, (3) 101468.
- Schwartz, M., 1971. Thymidine phosphorylase from *Escherichia coli*: properties and kinetics. *Eur. J. Biochem.* 21 (2), 191–198.
- Sharma, L.K. et al, 2010. Electrochemical synthesis of 5-substituted-2-amino-1,3,4-oxadiazoles at the llatinumelectrode. *Russ. J. Electrochem* 46, 34–40.
- Shivarama Holla, B., et al. (2005). “Synthesis and anticancer activity studies on some 2-chloro-1, 4-bis-(5-substituted-1, 3, 4-oxadiazol-2-ylmethyleneoxy) phenylene derivatives. *Indian J. Chem., Sect. B: Organic Chem. Including Med. Chem.* 44(8): 1669-1673.
- Taha, M. et al, 2017. Synthesis and molecular modelling studies of phenyl linked oxadiazole-phenylhydrazone hybrids as potent antileishmanial agents. *Eur. J. Med. Chem.* 126, 1021–1033.
- Ullah, H. et al, 2020. Aryl-oxadiazole Schiff bases: Synthesis,  $\alpha$ -glucosidase in vitro inhibitory activity and their in silico studies. *Arab. J. Chem.* 13 (4), 4904–4915.
- Usuki, K. et al, 1992. Platelet-derived endothelial cell growth factor has thymidine phosphorylase activity. *Biochem. Biophys. Res. Commun.* 184 (3), 1311–1316.
- Zheng, Z. et al, 2018. Antimicrobial activity of 1, 3, 4-oxadiazole derivatives against planktonic cells and biofilm of *Staphylococcus aureus*. *Future Med. Chem.* 10 (3), 283–296.
- Zhou, X., Shao, L., Jin, Z., Liu, J.B., Dai, H., Fang, J.X., 2007. Synthesis and antitumor activity evaluation of some schiff bases derived from 2-aminothiazole derivatives. *Heteroatom Chem.: An Int. J. Main Group Elements* 18 (1), 55–59.
- Zhu, W. et al, 2016. Design, synthesis, and pharmacological evaluation of 5-oxo-1, 2, 4-oxadiazole derivatives as AT1 antagonists with antihypertension activities. *Clin. Exp. Hypertens.* 38 (5), 435–442.